In the determination of wall heat flux, three different types of grid arrangements (namely, uniform, nonuniform, and deforming grids) were used in conjunction with the above-mentioned Newton-Raphson iteration procedure. An iterative index is included in the computer program to count the number of iterations necessary to achieve desired accuracy in the minimization of the function $|F|$. In each case, 11 nodes and a time interval of 1 s are taken for computational purposes. In the case of nonuniform grid, 5 meshes are stretched near the convectively heated surface of the slab while the remaining mesh covers the rest of the region. Figure 1 shows the mesh movement at each time interval using the heat penetration depth concept. The numerical computations have been performed on a CDC 170/730 digital computer. The convective heat-transfer coefficient can be calculated as

$$h = q_w/(T_{aw} - T_s) \tag{14}$$

where T_s is the surface temperature. Table 1 depicts predicted values of wall heat flux, surface temperature, and convective heat-transfer coefficient using the three different kinds of grid arrangements. It can be seen from the table that for $t \leq 6$ s, the heat-transfer coefficient obtained using the deforming grid strategy is in good agreement with the calculated results of Bartz.[11] Thus, the current numerical analysis shows that the moving-grid finite-element formulation gives an adequate modeling of the transient steep gradient of wall heat flux near the boundary of the heated surface. But for $t > 6$ s, fixed and deforming grid results tend to coincide since spatial grids become identical, as shown in Fig. 1. The estimated values of heat-transfer coefficient calculated using three different type of grid arrangements are somewhat lower than the calculated results of Bartz for $t > 6$ s. The predicted value of the heat-transfer coefficient shows that the Bartz equation gives a conservative estimation of the heat-transfer coefficient. This is also demonstrated in the previous analysis.[12] The maximum number of iterations per step are 11 and 8 for the uniform and nonuniform grids, respectively, whereas it is reduced to 4 iterations per step in the case of deforming grid. This example thus reveals that the deforming grid is economical in terms of CPU time compared to the other type of grid arrangements. This example also demonstrates that the arbitrary mesh deformation can be conveniently accommodated in the solution to the inverse problem of heat conduction. It is also important to mention here that geometrical conservation is maintained using nonuniform and deforming grids in the analysis because the numerical computations are carried out in the physical plane.

Conclusions

A mesh coupling thermal conductivity matrix with deforming finite-element formulation with heat penetration depth concept is found useful to treat the initial time delay in temperature response. The deforming grid procedure has shown itself to reduce substantially the number of iterations per step to achieve the required tolerance in the analysis of the inverse heat-conduction problem.

References

[1]Beck, J. V., Blackwell, B., and St. Clair, C. R. Jr., *Inverse Heat Conduction Problem*, Wiley, New York, 1985.

[2]Mehta, R. C., "An Efficient Numerical Method for Solving Inverse Heat Conduction Problem in a Hollow Cylinder," *AIAA Journal*, Vol. 22, June 1984, pp. 860–862.

[3]Bass, B. R., "Application of the Finite Element Method to the Nonlinear Inverse Heat Conduction Problem Using Beck's Second Method," *Journal of Engineering for Industry*, Vol. 102, May 1980, pp. 168–176.

[4]Lynch, D. R. and O'Neill, K. "Continuously Deforming Finite Elements for the Solution of Parabolic Problems, With and Without Phase Change," *International Journal for Numerical Methods in Engineering*, Vol. 17, 1981, pp. 81–96.

[5]Zienkiewicz, O. C., *The Finite Element Method in Engineering Science*, McGraw-Hill, London, 1971.

[6]Hogge, M. and Gerrekens, P., "Steep Gradient Modeling in Diffusion Problems", *Numerical Method in Heat Transfer II*, edited by R. W. Lewis, K. Morgan, and B. A. Schrefler, Wiley, New York, 1983, pp. 73–93.

[7]Lynch, D. R. and Gray, W. G., "Finite Element Simulation of Flow in Deforming Regions," *Journal of Computational Phyics*, Vol. 36, July 1980, pp. 135–153.

[8]Owen, D. R. J. and Damjanic, F., "The Stability of Numerical Time Integration Techniques for Transient Thermal Problems with Special Reference to Integration Effects," *Numerical Methods in Thermal Problems, Proceedings of the 2nd International Conference*, edited by R. W. Lewis, K. Morgan, and B. A. Schreffer, Pineridge Press, 1981, pp. 487–505.

[9]Mehta, R. C., "Numerical Solution of Nonlinear Inverse Heat Conduction Problem with a Radiation Boundary Condition," *International Journal for Numerical Methods in Engineering*, Vol. 20, 1984, pp. 1057–1066.

[10]Beck, J. V., "Nonlinear Estimation Applied to the Nonlinear Inverse Heat Conduction Problem," *International Journal of Heat and Mass Transfer*, Vol. 13, April 1970, pp. 703–716.

[11]Bartz, D. R., "A Simple Equation for Rapid Estimation of Rocket Nozzle Convective Heat Transfer Coefficients," *Jet Propulsion*, Vol. 27, Jan. 1957, pp. 49–51.

[12]Mehta, R. C., "Solution of the Inverse Conduction Problem," *AIAA Journal*, Vol. 15, Sept. 1977, pp. 1355–1356.

Approximate Method for Transient Conduction in Arbitrarily Shaped Solids with a Volumetric Heat Source

K. Taghavi* and R. A. Altenkirch†
University of Kentucky, Lexington, Kentucky

Introduction

THE lumped-heat-capacity technique has long been used to predict transient thermal behavior of solids when the Biot number is small compared to unity.[1] A small Biot number implies a negligible spatial temperature variation within the solid. This method, when applicable, is simple and powerful because it may be applied to any geometry.

In this work, a quasi-steady-state model is considered for solids with internal heat generation and arbitrary Biot number. It is assumed that the temperature profile in the solid at any instant in time is similar to that of the steady state. The basis of this approach has been explained by Arpaci[2] and parallels that for thermally fully developed internal flows. A fully developed regime has been identified for unsteady conduction in solids with convective boundary conditions, but without heat generation.[3] Here, we consider the presence of a heat source, the steady state becomes analogous to fully developed internal flow, and the temporal behavior of the temperature field is contained in the behavior of the mass-averaged (bulk) temperature. The approach will be shown to be more accurate than the lumped-heat-capacity technique and is easily applied to solids with arbitrary shapes.

Received April 10, 1987; revision received Jan. 29, 1988.

*Assistant Professor, Department of Mechanical Engineering.

†Professor, Department of Mechanical Engineering; currently at Department of Mechanical and Nuclear Engineering, Mississipi State University.

Analysis

The problem considered here is that of an arbitrarily shaped solid with a volumetric heat source Q that is exposed at its surface to a fluid at T_f with heat-transfer coefficient h. An overall energy balance on the solid of volume V and surface area A_s gives

$$\rho c_p V \frac{d\overline{T}}{dt} = hA_s(T_f - \overline{T}_s) + QV \tag{1}$$

where $\overline{T}$ is the volume-averaged temperature, and t is time. The average surface temperature $\overline{T}_s$ is defined as

$$hA_s(T_f - \overline{T}_s) = \int_{A_s} h(T_f - T_s)\, dA_s \tag{2}$$

In Eq. (1), ρ and c_p are the density and the specific heat of the solid. Equation (1) is exact; no approximation based on the magnitude of the Biot number has been introduced. To obtain a solution to Eq. (1), though, some knowledge of the relationship between $\overline{T}$ and $\overline{T}_s$ is needed. The shape of the temperature profile at any instant in time is taken to be similar to that of the steady-state solution (hence quasisteady approximation). By defining a temperature profile shape factor β as

$$\beta = (\overline{T} - T_f)/(\overline{T}_s - T_f) = (\overline{T}_\infty - T_f)/(\overline{T}_{s\infty} - T_f) \tag{3}$$

with the steady-state solution designated by a subscript ∞. Equation (1) can be written as

$$\rho c_p V \frac{d(\overline{T} - T_f)}{dt} = -hA_s\beta^{-1}(\overline{T} - T_f) + QV \tag{4}$$

Equation (3), which is useful in assessing the error in assigning $\overline{T} = \overline{T}_s$ for Biot numbers that are not small, approaches the lumped-heat-capacity condition in the limit as $Bi \rightarrow 0$. In this limit, $\beta \rightarrow 1$, $\overline{T}_s \rightarrow \overline{T}$, and the single-temperature approximation becomes exact. For example, Midkiff and Altenkirch[4] used Eq. (3), when applied to a spherical geometry, to approximate the error involved in taking the volatiles concentration within a devolatilizing coal particle to be uniform for mass transfer Biot numbers of order of unity.

Let $\overline{T}_o$ be the initial steady-state average temperature for a solid with an internal heat source Q_o. Also, let θ be $\overline{T} - \overline{T}_o$ such that a θ different from zero is due to a perturbation of Q_o equal to ΔQ at time zero. From Eq. (4), θ then satisfies

$$\rho c_p V \frac{d\theta}{dt} = -hA_s\beta^{-1}\theta + \Delta QV \tag{5}$$

with the initial condition

$$\theta = 0, \qquad \text{at } t = 0 \tag{6}$$

Equations (5) and (6) may be easily solved to obtain

$$\theta = \theta_\infty\left[1 - \exp\left(-\frac{Bi\,\tau}{\beta}\right)\right] \tag{7}$$

where θ_∞ is the steady-state solution for the perturbed volumetric heat source and may be obtained by setting $d\theta/dt = 0$ in Eq. (5) and solving for θ. Because θ_∞ is geometry-dependent, it is not given here in detail in order to maintain generality. The Biot number Bi and the dimensionless time τ in Eq. (7) are defined as

$$Bi = h\ell/k \tag{8}$$

$$\tau = \alpha t/\ell^2 \tag{9}$$

where k and α are the thermal conductivity and thermal diffusivity, and the characteristic length ℓ is defined as

$$\ell = V/A_s \tag{10}$$

Equation (7) can be rewritten in terms of a characteristic time as

$$\theta = \theta_\infty\,[1 - \exp(-\tau/\tau_c)] \tag{11}$$

where the characteristic time τ_c is defined as

$$\tau_c = \beta/Bi \tag{12}$$

The temperature profile shape factor may be calculated by invoking the energy balance at steady state.

$$hA_s(\overline{T}_{s\infty} - T_f) = QV \tag{13}$$

Substituting Eqs. (3) and (13) in Eq. (12) results in a relation for the characteristic time:

$$\tau_c = (\overline{T}_\infty - T_f)/(Q\ell^2/k) \tag{14}$$

Results and Discussion

Here we compare present technique to the lumped-heat-capacity method and to the exact results for the geometries of a slab, an infinite cylinder, and a sphere. For these standard geometries, exact solutions exist for the transient and the steady-state situations.[5] For these three geometries

$$\ell = R/m; \quad m = 1\text{:slab}, \quad 2\text{:cylinder}, \quad 3\text{:sphere} \tag{15}$$

where R is the slab half-thickness or the radius of the cylinder or the sphere; the characteristic time is

$$\tau_c = Bi^{-1} + [m/(m+2)] \tag{16}$$

Uniform Heat Source

Figures 1–3 show the normalized, average temperature as a function of dimensionless time for three values of the Biot number for a slab. No result is given for Biot numbers less than unity because both the present technique and that of lumped-heat-capacity compare favorably with the exact solution. In Fig. 1, the exact result and the present work coincide within the resolution of the line drawing. The maximum difference between these two is less than 1%. It is seen from these figures that the present results compare rather satisfactorily with the exact results, whereas the lumped-heat-capacity model does not compare well with either as the Biot number is

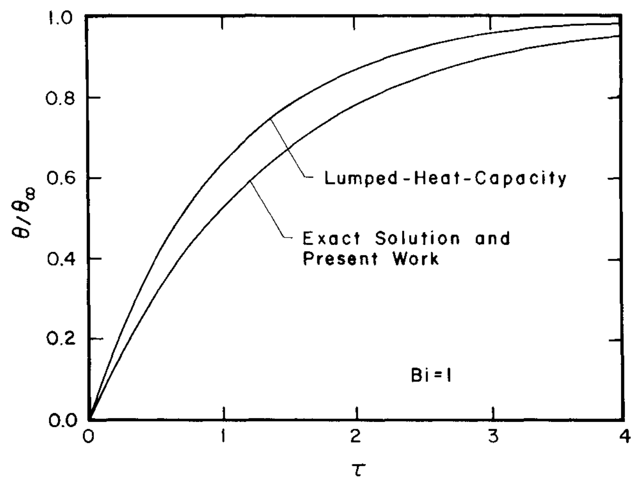

Fig. 1 Average temperature as a function of time for a slab for $Bi = 1$.

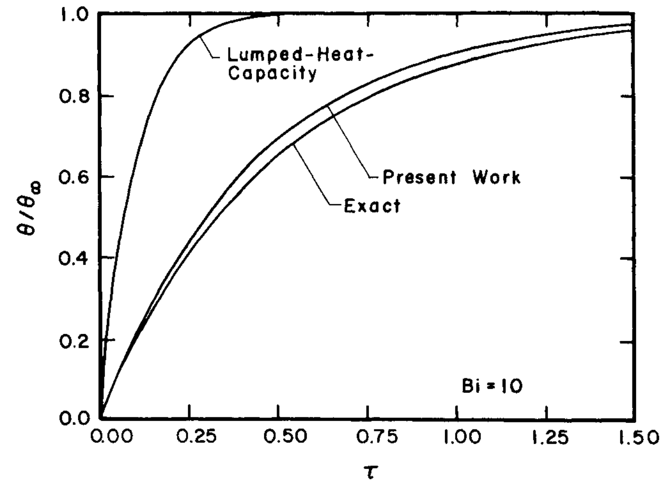

Fig. 2 Average temperature as a function of time for a slab for $Bi = 10$.

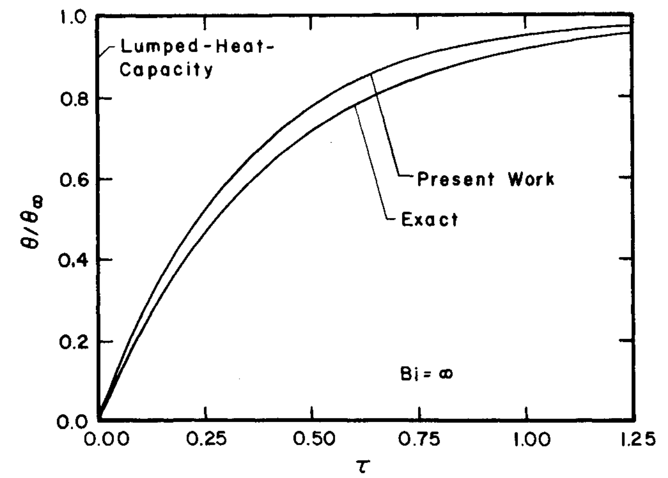

Fig. 3 Average temperature as a function of time for a slab for $Bi \to \infty$.

increased. For example, a Biot number of 10, at a dimensionless time of 0.25, the lumped-heat-capacity method predicts results more than 100% larger than the exact analysis, whereas the present work gives a result that is only 6.7% larger than the exact result. This agreement becomes less satisfactory as the Biot number increases. The difference between the present work and the exact solution, however, is bounded as the Biot number approaches infinity. Figure 3 shows the results for a Biot number of infinity, which implies that the boundary condition at the interface is one of prescribed temperature rather than of heat convection. It is seen from this figure that the present technique is satisfactory even for an infinitely large Biot number.

Results similar to Figs. 1–3 have also been obtained for an infinite cylinder and a sphere. The general trend is the same as for a slab. The agreement between the present work and the exact results, however, is slightly better for a slab than it is for an infinite cylinder or a sphere. To show this more clearly, Fig. 4 depicts the difference between the present technique and the exact result as a function of dimensionless time for all the geometries considered here. Figure 4 is drawn for an infinitely large Biot number where the error is largest. It is seen from the figure that the present technique is most accurate for the slab geometry, and the largest error at any time is less than 25%. A typical error is about 5–10%.

The fact that the present method yields satisfactory results indicates that an approximate similarity exists in the transient behavior of solids with an internal heat source. That is to say,

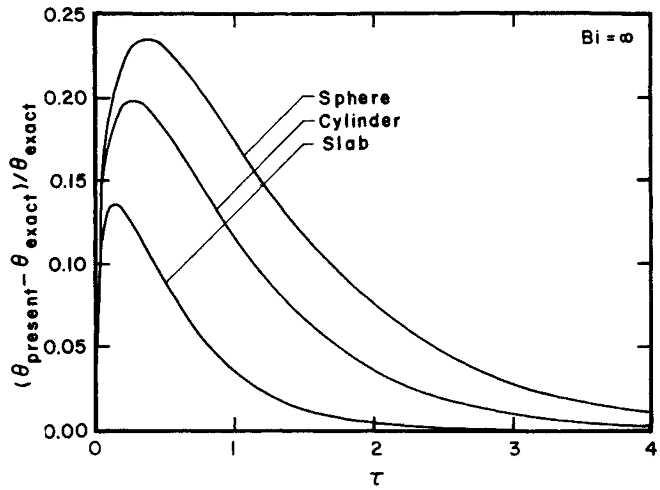

Fig. 4 Comparison of the present approximate method with the exact solutions for a sphere, an infinite cylinder, and a slab for $Bi \to \infty$.

the temperature profile at any time may be written approximately as

$$T(x,\tau) - T(x,0) \simeq [T(x,\infty) - T(x,0)]\,[1 - \exp(-\tau/\tau_c)] \quad (17)$$

where $T(x,\infty)$ is the steady-state temperature profile.

Nonuniform Heat Source

Equation (14) is valid for the case of a uniform heat source. It is useful to examine the accuracy and applicability of this equation to cases with a nonuniform heat source. For the purpose of illustration, we examine here the approximate equation governing thermal explosions.[6,7] In this equation, the heat source varies exponentially with the temperature according to

$$Q \simeq \delta \exp(\theta) \quad (18)$$

where δ is the pre-exponential factor (Damköhler number). For this heat-source distribution, we no longer can use Eq. (14) unless Q is replaced by some average heat source. Alternatively, we may use Eq. (3) to evaluate β and use Eq. (12) to calculate the characteristic time τ_c.

To apply the present technique to the thermal explosion problem, we need the steady-state temperature profile. The conduction equation with a heat-source term of the form of Eq. (18) does not admit a closed-form solution, and so we solved it numerically. Once the steady-state profile is known, the characteristic time may be calculated from Eqs. (12) and (3).

Figure 5 shows the result of such a calculation. It is seen that the characteristic time is not strongly dependent on the coefficient in the heat-source term, indicating that Eqs. (16) and (17) also hold for the case of a nonuniform heat source. As δ approaches zero, the characteristic time approaches that obtained from Eq. (16). It may be noted that above some δ, no steady-state solution exists, and thermal runaway or explosion occurs.[7] No results are given beyond these values of δ, which may be found in Glassman.[6]

Other Geometries

An interesting feature of this method is that it may be easily applied to irregular geometries. To demonstrate the applicability of the present technique to irregular shapes, a parallelepiped with variable aspect ratio a is selected. In performing the comparison between the present method, the exact results, and the lumped-heat-capacity technique, we also choose for comparison two traditional approximate methods normally used with irregular shapes.

The first method is inspired by the product rule applied in transient conduction.[1] An infinite parallelepiped with dimen-

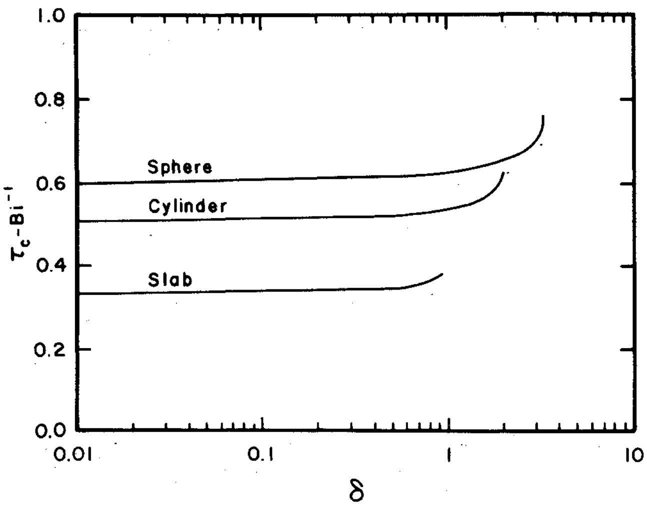

Fig. 5 Characteristic time for a nonuniform heat source $Q = \delta \exp(\theta)$.

sions of $1 \times a$ is divided into two infinite slabs with dimensions of 1 and a (say in the x and y directions). Subsequently, the characteristic time of each slab is calculated from Eq. (16), noting that these times are based on different characteristic lengths. Once converted to dimensionless times based on the characteristic length of the parallelepiped, the product rule may be written as

$$\tau_c^{-1} = \tau_{c,x}^{-1} + \tau_{c,y}^{-1} \tag{19}$$

where $\tau_{c,x}$ and $\tau_{c,y}$ are the characteristic times for the infinite slabs in the x and y directions. Before applying the product rule to our present technique, we should examine its accuracy. We compared the exact solution for a parallelepiped of dimensions $1 \times a$ with the product rule [Eq. (19)] applied to the exact solution for two slabs with dimensions 1 and a. The maximum error, over the range of $a = 1 \rightarrow \infty$, was less than 7% with a typical error of less than 2%. This excellent agreement suggests that the product rule, although not exact, is a good approximation.

Next, we apply the product rule to the present technique. For the particular case of an infinite parallelepiped with an aspect ratio of a and $Bi \rightarrow \infty$, Eqs. (16) and (19) yield

$$\tau_c = (a+1)^2/[3(a^2+1)], \qquad \text{for } Bi \rightarrow \infty \tag{20}$$

Equation (20) is shown in Fig. 6. In this figure, the exact characteristic time, obtained numerically, is plotted as a function of aspect ratio for an infinitely large Biot number. As can be seen, Eq. (20) is close to the exact result; the maximum error is about 15%.

A second method that may be used to circumvent the requirement that the steady-state temperature for a particular geometry be known, is to equate any geometry to one of the more common geometries, i.e., a slab, an infinite cylinder, or a sphere, while maintaining a constant characteristic length ℓ. The result of such an approximation for a parallelepiped is shown in Fig. 6. In this figure, the constant-ℓ approximation, i.e., equating a parallelepiped to an infinitely long slab while keeping the characteristic length ℓ constant, is shown. Although the approximation is more satisfactory for large aspect ratios, it results in large errors (as much as 100%) for small aspect ratios. It should be mentioned that the lumped-heat-capacity method yields $\tau_c \rightarrow \infty$ for $Bi \rightarrow \infty$.

Figure 6 also includes the present approximation, Eq. (14), applied to a rectangular parallelepiped. It is seen that the present method is in good agreement with the exact results. Although the product rule seems to be a better approximation,

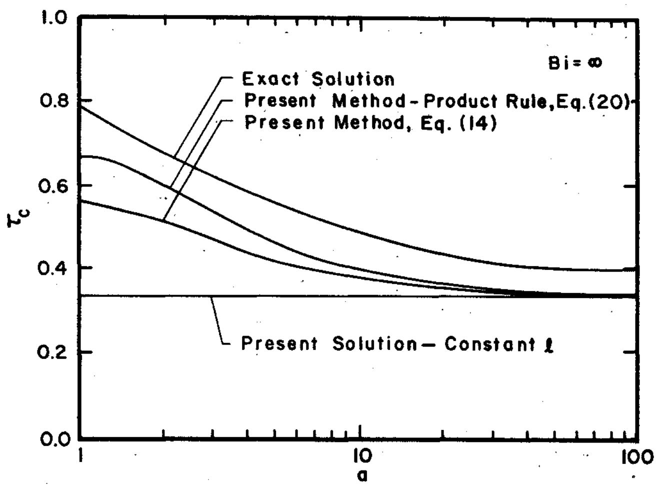

Fig. 6 Comparison of the present, approximate method with the exact solution for an infinite parallelepiped for $Bi \rightarrow \infty$.

it should be noted that the product rule is applicable only to those geometries that are separable into standard geometries for which exact steady-state solutions are available. The present technique, however, applies to any geometry and only requires information regarding the steady-state average temperature.

Summary and Conclusions

A method has been presented that allows the transient thermal behavior of solids with an internal heat source to be predicted approximately for any Biot number. The method, similar to that used for thermally fully developed internal flows, is an improvement over the lumped-heat-capacity approximation in that it yields satisfactory results, even for large Biot numbers, where the lumped-heat-capacity approximation is not valid. Although development of the method requires that the heat source be uniform throughout the solid, results computed for a nonuniform heat source appear to be satisfactory. A treatment similar to the well-known product rule used in transient conduction is introduced in order to extend application of the method to geometries other than those of a slab, an infinite cylinder, or a sphere. The present method was also tested for irregular geometries, and the comparison with the exact solution was satisfactory.

Acknowledgment

We thank John H. Lienhard and Eugene Ungar for reading the initial draft of the manuscript and offering some useful criticism.

References

[1]Lienhard, J. H., *A Heat Transfer Textbook*, 2nd ed., Prentice-Hall, Englewood Cliffs, NJ, 1981.

[2]Arpaci, V. S., *Conduction Heat Transfer*, Addison-Wesley, Reading, MA, 1966.

[3]Patankar, S. V., "The Concept of a Fully Developed Regime in Unsteady Heat Conduction," *Studies in Heat Transfer: A Festschrift for E. R. G. Eckert*, edited by J. P. Hartnett, T. F. Irvine Jr., E. Pfender, and E. M. Sparrow, McGraw-Hill, New York, 1979, pp. 419–431.

[4]Midkiff, K. C. and Altenkirch, R. A., "Particle-Size Effects on the Distribution of Fuel Nitrogen in One-Dimensional Coal-Dust Flames," *Twenty-First Symposium (International) on Combustion*, The Combustion Institute, Pittsburgh, PA, 1988, pp. 1189–1198.

[5]Carslaw, H. S. and Jaeger, J. C., *Conduction of Heat in Solids*, 2nd ed., Oxford University Press, Oxford, 1959.

[6]Glassman, I., *Combustion*, Academic Press, New York, 1977.

[7]Williams, F. A., *Combustion Theory*, 2nd ed., Benjamin/Cummings, Menlo Park, CA, 1985.